Kamaris, GS, Vallianatou, YM and Beskos, DE

Seismic damage estimation of in-plane regular steel moment resisting and x-braced frames

Seismic damage estimation of in-plane regular steel moment resisting and x-braced frames

George S. Kamaris[a], Yasemi-Maria Vallianatou[a] and Dimitri E. Beskos[a,b,*]

[a] Department of Civil Engineering, University of Patras, GR- 26500 Patras, Greece

[b] Office of Theoretical and Applied Mechanics, Academy of Athens, 4 Soranou Efessiou, GR-11527 Athens, Greece.

Abstract: Simple empirical expressions to estimate maximum seismic damage on the basis of five well known damage indices for planar regular moment resisting and x-braced steel frames are presented. They are based on the results of extensive parametric studies concerning the inelastic response of a large number of these frames to a large number of ground motions. Thousands of nonlinear dynamic analyses are performed by scaling the seismic records to different intensities in order to drive the structures to different levels of inelastic deformation and finally to collapse. The statistical analysis of the created response databank indicates that the number of stories, period of vibration, stiffness ratio, capacity factor (for moment resisting frames), brace slenderness ratio and column stiffness (for x-braced frames) and characteristics of the ground motion, such as characteristic period and spectral acceleration, strongly influence damage. Nonlinear regression analysis is employed in order to derive simple formulae, which reflect the influence of the aforementioned parameters and offer a direct estimation of the damage indices used in this study. More specifically, given the characteristics of the structure and the ground motion, one can calculate the maximum damage observed in column bases and beams (for moment resisting frames) or in braces (for x-braced frames). Finally, two examples serve to illustrate the use of the proposed expressions and demonstrate their accuracy and efficiency.

Keywords: Steel moment resisting frames; x-braced steel frames; Damage indices; Seismic assessment; Ordinary ground motions.

[*]: Corresponding author: Tel.: +30.2610.996559; Fax: +30.2610.996579
E-mail address: d.e.beskos@upatras.gr

1. Introduction

Damage in a structure under loading can be defined as the degradation or deterioration of its integrity resulting in reduction of its load capacity. In earthquake-resistant design of structures, some degree of damage in the structural members is generally accepted. This is done because the cost of a structure designed to remain elastic during a severe earthquake would be very large. Thus, existing seismic codes, e.g., EC8 [1], in an implicit way and more recent performance-based seismic design methods [2,3] in an explicit and more systematic way employ the concept of damage to establish structural performance levels corresponding to increasing levels of earthquake actions. These performance levels mainly describe the damage of a structure through damage indices, such as the interstory drift ratio (IDR), or the member plastic rotations.

Several methods to determine damage indices as functions of certain response parameters have been presented in the literature. In general, these methods can be noncumulative or cumulative in nature. The most commonly used parameter of the first class is ductility, which relates damage only to the maximum deformation and is still regarded as a critical design parameter by codes. To account for the effects of cyclic loading, simple rules of stiffness and strength degradation have been included in various noncumulative indices [4,5,6], mainly referred to reinforced concrete members. Cumulative-type indices can be divided in deformation based [7] or hysteresis based [8,9] formulations and methods that consider the effective distribution of inelastic cycles and generalize the linear law of low-cycle fatigue of metals through a hypothesis of linear damage accumulation [10]. Sucuoğlu and Erberik [11] developed low-cycle fatigue damage models for deteriorating systems on the basis of test data and analysis and Kamaris et al. [12] proposed a new damage model exhibiting strength and stiffness degradation which takes into account the phenomenon of low-cycle fatigue and the interaction between axial force and bending moment at a section of a beam-column steel member. Combinations of deformation and energy dissipation have been also proposed to establish damage indices [13]. In these methods damage is expressed as a linear combination of the damage caused by excessive deformation and that due to repeated cyclic loading effects [13]. An extensive review of damage indices used in the literature can be found in Powell and Allahabadi [14]. Finally, the concept of continuum damage mechanics [15] in conjunction with the finite element method of concentrated inelasticity has been employed in the analysis of steel and reinforced concrete structures [16,17] for the determination of their damage.

The goal of this paper is to study the seismic inelastic behavior of plane steel moment resisting frames (MRF) and x-braced frames (XBF) and quantify their damage through simple expressions that relate the most commonly used damage indices of the literature with the characteristics of the frames and the ground motions. For that purpose, a large number of steel MRF and steel XBF are

subjected to an ensemble of 40 ordinary (i.e. without near-fault effects) ground motions scaled to different intensities. A response databank is created and a regression analysis is performed in order to derive simple formulae that can be used for the prediction of damage. Two examples are utilized to illustrate the use of the proposed formulae and demonstrate their efficiency and accuracy. It should be pointed out that the seismic damage calculated herein is "probably expected" and not a deterministic damage value, since the procedures utilized in this paper are based on statistical formulae.

The proposed methodology provides the means of a rapid and accurate damage assessment of existing structures, avoiding the use of the more sophisticated and time consuming non-linear dynamic analysis. It can also be utilized in the preliminary design of structures in the framework of a performance based design approach in order to size a frame to achieve a preselected damage level. Thus, the designer can perform a preliminary design of high quality based on elastic analysis and the proposed relationships, which can significantly decrease the need for iterations of analysis/design. This is very important when analysis is non-linear dynamic and time consuming. In addition, the proposed equations can be used in conjunction with a pushover analysis. This kind of analysis, when it is performed up to a target displacement, cannot predict cyclic accumulated damage, something that can be fulfilled only by damage indices. Therefore, the proposed expressions can be useful even in this case. Finally, the main advantages of the proposed formulae is rapidness, simplicity and accuracy, since one can compute very easily, quantities such as damage indices, which can only be found by more advanced methods.

2. Damage indices used in this study

The proposed damage expressions are associated with five damage indices existing in the literature. These are the damage indices of Park and Ang [13], Bracci et al. [9], Roufaiel and Meyer [5], Cosenza et al. [6] and Banon and Veneziano [4]. These indices have been selected here because i) are the most widely used in applications and ii) can be easily employed with the aid of the Ruaumoko 2D program [18]. In the following, a brief description of all these five damage indices will be given for reasons of completeness.

The damage index D_{PA} of Park and Ang [13] is expressed as a linear combination of the damage caused by excessive deformation and that contributed by repeated cyclic loading effects, as shown in the following equation:

$$D_{PA} = \frac{\delta_m}{\delta_u} + \frac{\beta}{Q_y \delta_u} \int dE \qquad (1)$$

In the above, the first part of the index is expressed as the ratio of the maximum experienced deformation δ_m to the ultimate deformation δ_u under monotonic loading. The second part is defined as the ratio of the dissipated energy $\int dE$ to the term $(Q_y\,\delta_u)/\beta$, where Q_y is the yield strength and the coefficient β is a non-negative parameter determined from experimental calibration. In this paper β is taken equal to 0.025, which is a typical value for steel structures [19].

Bracci et al. [9] suggested a damage index equal to the ratio of 'damage consumption' (loss in damage capacity) to 'damage potential' (capacity), defined as appropriate areas under the monotonic and the low-cycle fatigue envelopes. Thus, the 'damage potential' D_P is defined as the total area between the monotonic load–deformation curve and the fatigue failure envelope. As damage proceeds, the load–deformation curve degrades, resulting in the damage D_s due to the loss of strength, while the irrecoverable deformation causes the deformation damage D_D. Thus, this damage index D_{BRM} is expressed as

$$D_{BRM} = \frac{D_D + D_S}{D_P} \tag{2}$$

Roufaiel and Meyer [5] proposed that the ratio between the secant stiffness at the onset of failure M_m/ϕ_m and the minimum secant stiffness reached so far M_x/ϕ_x, can be used as a good indicator of damage. Based on that, they defined the modified flexural damage ratio (MFDR) or D_{RM} as

$$D_{RM} = MFDR = \max[MFDR^+, MFDR^-] \tag{3}$$

$$MFDR^+ = \frac{\phi_x^+}{M_x^+} - \frac{\phi_y^+}{M_y^+} \Bigg/ \frac{\phi_m^+}{M_m^+} - \frac{\phi_y^+}{M_y^+}, \quad MFDR^- = \frac{\phi_x^-}{M_x^-} - \frac{\phi_y^-}{M_y^-} \Bigg/ \frac{\phi_m^-}{M_m^-} - \frac{\phi_y^-}{M_y^-} \tag{4}$$

where ϕ is the beam curvature due to a bending moment M, the term M_y/ϕ_y is the initial elastic stiffness and subscripts + and – denote the loading direction.

The Consenza et al. [6] damage index is defined as

$$D_{CMR} = \frac{\mu - 1}{\mu_{u,mon} - 1} \tag{5}$$

where μ is the maximum ductility during the loading history and $\mu_{u,mon}$ is the maximum allowable value of ductility equal to $x_{u,mon}/x_y$ with the $x_{u,mon}$ being the ultimate displacement given

by monotonic tests and x_y the yield displacement. For members that are under flexure, μ, $\mu_{u,mon}$, $x_{u,mon}$ and x_y are replaced by μ_θ, $\mu_{\theta,mon}$, $\theta_{u,mon}$, and θ_y, respectively. The terms μ_θ, $\mu_{\theta,mon}$ are the rotation ductility during the loading history and the maximum allowable value of rotation ductility under monotonic tests, respectively, while $\theta_{u,mon}$, and θ_y are the ultimate and the yield rotation, respectively.

The Banon and Veneziano [4] analysis is set in a probabilistic context and their model has been calibrated on the basis of 29 different tests on reinforced concrete elements and structures, selected from among the most representative ones in the technical literature. In particular, the damage parameters d_l and d_2 are defined, respectively, as the ratio of stiffness at yielding point to secant stiffness at failure, and the plastic dissipated energy E_h normalized with respect to the absorbed energy at the elastic limit. If the elastic-plastic model is used, d_1 is obviously equal to the ratio of the maximum displacement x_{max} to the displacement at the elastic limit x_y. Therefore, according to the notation introduced above, parameters d_1 and d_2 can be expressed as

$$d_1 = x_{max} / x_y , \quad d_2 = E_h / \left(1/2\right) F_y x_y \tag{6}$$

where F_y is the yield strength. Furthermore, modified damage parameters d_1^* and d_2^* are introduced of the form

$$d_1^* = d_1 - 1 \tag{7}$$

$$d_2^* = a d_2^b \tag{8}$$

where a and b are two parameters which characterize the structural problem and are defined experimentally. For flexure, x and F are replaced by θ and M, respectively. Thus, the damage index D_{BV} is defined as

$$D_{BV} = \sqrt{(d_1^*)^2 + (d_2^*)^2} \tag{9}$$

3. Frames considered in this study

3.1 Moment resisting frames

In order to cover a wide range of structural characteristics of steel moment resisting frames (MRF), a family of 54 plane steel MRF was employed for the parametric studies of this work. These frames are regular and orthogonal with storey heights and bay widths equal to 3 m and 5 m, respectively (Fig. 1). Furthermore, they have the following characteristics: number of stories n_s with values 3, 6, 9, 12, 15, and 20; number of bays n_b with values only 3 and 6 since it was found from preliminary studies that n_b has a negligible effect on damage; beam-to-column stiffness ratio, ρ, with various values within practical limits.

The stiffness ratio ρ of a frame is calculated for the storey closest to the mid-height of the frame via the expression

$$\rho = \frac{\sum (I/l)_b}{\sum (I/l)_c} \tag{10}$$

where I and l are the second moment of inertia and length of the steel member (column c or beam b), respectively. The parameter ρ definitely controls the behavior of the frame in the elastic range of the response [20]. As ρ increases, the behavior of the frame moves from pure flexural (ρ = 0.0) to pure shear ($\rho = \infty$) behavior. In the inelastic range of the response and especially at higher values of ductility, the influence of ρ is lost since the structure behaves in a mechanism type of mode. The complete formation of a mechanism is achieved when plastic hinges are developed at the base of columns and at the ends of beams. According to this work, a parameter that influences the inelastic seismic response of steel MRF is the capacity factors α which is defined as

$$\alpha = M_{RC,1,av} / M_{RB,av} \tag{11}$$

where $M_{RC,1,av}$ is the average of the plastic moments of resistance of the columns of the first storey and $M_{RB,av}$ is the average of the plastic moments of resistance of the beams of all the stories of the frame.

Gravity load on the beams is assumed to be equal to 27.5 KN/m (dead and live loads of floors), while the yield stress of steel was set equal to 235 MPa. The frames have been designed in accordance with the provisions of structural Eurocodes EC3 [21] and EC8 [1]. The expected design

ground motion was defined by the acceleration response spectrum of EC8 [1] with a peak ground acceleration equal to 0.35 g, a soil class B and a behavior factor equal to 4.0. Data of the frames, including values for n_s, n_b, a_{cv}, beam and column sections and first and second natural periods, are presented in Table 1 taken from [22] and reproduced here for reasons of completeness. In that table, expressions of the form, e.g., 260–360(1–4) + 240–330(5–6) mean that the first four stories have columns with HEB260 sections and beams with IPE360 sections, whereas the next two higher stories have columns with HEB240 sections and beams with IPE330 sections [23].

3.2 X-braced frames

The 54 x-braced frames (XBF), considered here are plane, orthogonal and regular with storey heights and bay widths equal to 3 and 6 m, respectively (Fig. 2). The columns are pinned at their base but capable of carrying moments along the whole height of the building, while beams are shear connected to the columns. This assumption of pin connections between the framing members is widely accepted, although the presence of gusset plates increases the stiffness and hence decreases the inelastic deformation demands.

Gravity load on the beams is assumed equal to 27.5 kN/m (dead and live loads of floors), while the yield stress of the material is set equal to 235MPa. The frames are designed in accordance with the structural Eurocode EC3 [21] on the basis of a multi-mode response spectrum analysis and the assumption of a tension-compression (T/C) system for which the design storey shear is assumed to be equally resisted by both the tension-acting and the compression-acting diagonals and thus, the buckling axial resistance governs the selection of the required brace cross-section. The expected ground motion is defined by the elastic acceleration response spectrum of the EC8 [1] seismic code, with a peak ground acceleration equal to 0.35 g, a soil class B and a behavior factor q equal to 4.0. Commercially available cross-sections [23] were adopted in order to avoid discrepancies between strength, stiffness and slenderness which may arise from the use of fictitious sections. In particular, HEB, IPE and tube (TUBO) sections were used for the columns, beams and braces of the frames, respectively.

The number of stories, n_s, of the frames takes the values 3, 6, 9, 12, 15 and 20. For each frame corresponding to a n_s, three design processes were performed in order to obtain three distinct values (1.3, 1.56 and 1.93) of the brace slenderness, λ, defined as

$$\lambda = \frac{l}{\pi \cdot r}\sqrt{\frac{f_y}{E}} \tag{12}$$

where l is the buckling length, r is the radius of gyration of the cross-section, f_y is the yield strength of the material and E is Young's modulus. The effect of column stiffness [24, 25] is described by the ratio, α, of the contribution of the columns over that of the diagonals to the stiffness of a particular storey, i.e.,

$$\alpha = \frac{n_c \cdot I_c \cdot L_d}{n_d \cdot A_d \cdot h^3 \cdot \cos^2 \theta} \tag{13}$$

where n_c and n_d are the number of columns and diagonals belonging to that storey, respectively, A_d and L_d are the cross-sectional area and the length of the diagonals, respectively, I_c is the second moment of inertia of the columns, h is the storey height and θ the angle between diagonals and beams.

The design process for a specific combination of n_s, and λ resulted in cross-sections of the columns that provide the minimum strength and stiffness in order to avoid buckling and to remain elastic according to the code-dictated capacity design rules. The efficiency of the capacity design has been checked by performing a first-mode pushover analysis which revealed that no plastic hinges or buckling occur in columns at the ultimate limit state. For each of the frames, the column cross-sections were subsequently increased two times in order to obtain three different values of the parameter α. These values are not the same for all buildings since the effect of gravity loads on the selection of column section increases with an increasing number of stories. Both of the parameters λ and α vary along the height of the frame and therefore, their nominal values were calculated for the storey closest to the mid-height of the frame.

The aforementioned process led to a family of 6(n_s) 3(λ) 3(α) = 54 x-braced frames (XBF), which allows the study of the seismic damage observed at XBF with variations in their four structural characteristics n_s, α, λ and T. Data of the frames, including nominal values for n_s, α, λ and T as well as the sections of the columns and braces are depicted in Table 2 taken from [26,27] and reproduced here for reasons of completeness. The beam sections consist of standard IPE300 sections. In that table, expressions of the form, e.g., 220+220+220 mean that the first story has columns with HEB220 cross-sections, the second one has columns with HEB220 cross-sections whereas the third one has columns with HEB220 cross-sections.

4. Ground motions considered

In this work, a set of 40 physical ground motions, selected from the PEER [28] ground motion database, were employed for the nonlinear dynamic analyses. This set contains only far-fault

ground motions, i.e., motions recorded at a distance more than 15 km from the causative fault. The date, the record name, the excitation component, the peak ground acceleration, PGA, and the characteristic period, T_c, of the motions considered here are all provided in Table 3. Their elastic response spectra are portrayed in Fig. 3, where the median spectrum is shown by a thick line. Their characteristic period was calculated by employing the iterative algorithm of Riddell and Newmark [29] that divides the response spectrum into three period ranges: constant spectral displacement (long periods), constant spectral acceleration (short periods) and constant spectral velocity (intermediate periods). In order to cover the whole deformation range from elastic behavior up to collapse, all the aforementioned ground motions were scaled appropriately as explained in the next section.

5. Methodology for computation of damage expressions

In the present work, an extensive parametric study was conducted for the 54 plane steel MFR of Table 1 and the 54 plane steel XBF of Table 2, which were subjected to the 40 ground motions of Table 3 for the evaluation of the damage expressions. The frames were analyzed with the program Ruaumoko 2D [18] using the incremental dynamic analysis method. Thus, 21600 analyses (=54 frames x 40 ground motions x 10 analyses on the average for every frame) were conducted in this work for MRFs and XBFs. These 10 on the average analyses for every frame correspond to 10 different PGA values for every ground motion. The mathematical models of the frames were based on centerline representations with inelastic behavior of beams and columns modelled by means of bilinear (hysteretic) point plastic hinges with 3% hardening. The braces of the steel frames were simulated by the Remennikov and Walpole [30] model. These models do not incorporate the strength and stiffness of the panel zone. The panel zone area dimensions were not considered in the analysis. In addition, connections were assumed to be rigid. Finally, diaphragm action was assumed at every floor due to the presence of the slab.

The ground motion intensity level was measured here by an intensity measure (IM) equal to the spectral acceleration S_a, of the motion corresponding to the fundamental period of each frame. The structural response was measured by a damage measure (DM) equal to the maximum damage index among all storeys that was recorded during the time history of the analysis. More specifically, each ground motion was continuously scaled by increasing its S_a until the frame to become dynamically unstable and collapse. The results of the analysis were post-processed in order to create a databank with the response quantities of interest.

The created databank is actually a spreadsheet with rows equal to the number of nonlinear analyses and columns equal to the response quantities of interest in columns and beams of a MRF

or at braces of an x-braced frame along its height. Those response quantities are the maximum values of the following damage indices:1) Park and Ang damage index, D_{PA}, 2) Bracci et al. damage index, D_B, 3) Roufaiel and Meyer damage index, D_{RM}, 4) Cosenza et al. damage index, D_{CMR} and 5) Banon and Veneziano damage index, D_{BV}. Moreover, the columns of the databank were increased by adding the characteristics of the frames (n_s, ρ, α) and (n_s, λ, α) for MRFs and XBFs, respectively, the ratio of the fundamental period of vibration over the characteristic period of the ground motion, T/T_c and the spectral acceleration S_a.

6. Damage formulae for moment resisting frames

In this section, simple formulae to estimate seismic damage, through five well known damage indices, of planar regular steel MRFs are proposed. Thus, with the aid of these simple expressions one can determine the maximum damage of column bases or beams, D, of this type of frames in terms of characteristics of the structure and the ground motions that excite them.

By analyzing the response databank, no effect of the of the ratio T/T_c to the proposed relationship was identified and thus the expression

$$D = b_1 \cdot n_s^{b_2} \cdot \rho^{b_3} \cdot \alpha^{b_4} \cdot \left(\frac{S_a}{g} \right)^{b_5} \tag{14}$$

with b_1, b_2, b_3, b_4 and b_5 constants to be determined, was selected as a good candidate for approximating the response databank. The aforementioned relation is relatively simple and satisfies the physical constraint $D=0$ for $S_a=0$. Use of the Levenberg–Marquardt algorithm [31] for nonlinear regression analysis of the results of parametric studies, led to the following expressions for each one of the five damage indices

a) for column bases:

$$D_{PA}^{c} = 0.169 \cdot n_s^{0.181} \cdot \rho^{0.019} \cdot \alpha^{-0.051} \cdot \left(\frac{S_a}{g} \right)^{0.191} \tag{15}$$

$$D_{BRM}^{c} = 0.139 \cdot n_s^{0.530} \cdot \rho^{-0.026} \cdot \alpha^{0.010} \cdot \left(\frac{S_a}{g} \right)^{0.364} \tag{16}$$

$$D_{RM}^{c} = 0.097 \cdot n_s^{0.393} \cdot \rho^{-0.013} \cdot \alpha^{0.315} \cdot \left(\frac{S_a}{g} \right)^{0.097} \quad (17)$$

$$D_{CMR}^{c} = 0.104 \cdot n_s^{0.243} \cdot \rho^{0.006} \cdot \alpha^{0.007} \cdot \left(\frac{S_a}{g} \right)^{0.290} \quad (18)$$

$$D_{BV}^{c} = 0.212 \cdot n_s^{0.249} \cdot \rho^{-0.005} \cdot \alpha^{-0.128} \cdot \left(\frac{S_a}{g} \right)^{0.212} \quad (19)$$

b) for beams:

$$D_{PA}^{b} = 0.262 \cdot n_s^{0.326} \cdot \rho^{-0.013} \cdot \alpha^{-0.059} \cdot \left(\frac{S_a}{g} \right)^{0.351} \quad (20)$$

$$D_{BRM}^{b} = 0.179 \cdot n_s^{0.355} \cdot \rho^{-0.030} \cdot \alpha^{-0.007} \cdot \left(\frac{S_a}{g} \right)^{0.432} \quad (21)$$

$$D_{RM}^{b} = 0.215 \cdot n_s^{0.363} \cdot \rho^{0.014} \cdot \alpha^{0.023} \cdot \left(\frac{S_a}{g} \right)^{0.421} \quad (22)$$

$$D_{CMR}^{b} = 0.164 \cdot n_s^{0.388} \cdot \rho^{0.006} \cdot \alpha^{-0.069} \cdot \left(\frac{S_a}{g} \right)^{0.376} \quad (23)$$

$$D_{BV}^{b} = 0.317 \cdot n_s^{0.325} \cdot \rho^{0.035} \cdot \alpha^{0.036} \cdot \left(\frac{S_a}{g} \right)^{0.388} \quad (24)$$

With D being any damage index of interest, the mean, median and standard deviation of the ratio of the "exact" value of D obtained from inelastic dynamic analyses over the approximate one calculated from Eqs (15) to (24), respectively., i.e., D_{exact}/D_{app}, are used in order to express the central tendency and the dispersion of the error introduced by the proposed relations. Thus, for the Park and Ang [13] damage index, the ratio $D_{PA,c.exact}/D_{PA,c,app}$, for column bases, corresponds to a mean value equal to 0.99, a central value equal to 0.98 and a standard deviation equal to 0.30. Furthermore, this ratio corresponds to a mean value equal to 0.98, 0.99, 0.99 and 0.99, a central value equal to 0.93, 0.96, 0.97 and 0.99 and a standard deviation equal to 0.31, 0.45, 0.44 and 0.33 for the Bracci et al. [9], Roufaiel and Meyer [5], Cosenza et al. [6] and Banon and Veneziano [4] damage indices, respectively. The above ratio for beams corresponds to a mean value equal to 0.98, 0.96, 0.96, 0.97 and 0.98, a central value equal to 0.98, 0.95, 0.97, 0.99 and 0.99 and a standard deviation equal to 0.26, 0.36, 0.36, 0.37 and 0.26 for the Park and Ang [13], the Bracci et al. [9], Roufaiel and Meyer [5], Cosenza et al. [6] and Banon and Veneziano [4] damage indices, respectively. Those values show that the proposed formulae are of high accuracy.

7. Damage formulae for x-braced frames

In this section, simple expressions to estimate seismic damage, through five well known damage indices, of planar regular steel XBFs are proposed. Thus, with the aid of these simple expressions one can determine the maximum damage of the braces, D, of this type of frames in terms of characteristics of the structure and the ground motions that excite them. Such characteristics are the number of storeys, n_s, the brace slenderness, λ, the ratio α, the fundamental period of the frame, T , the spectral acceleration S_a and the characteristic period of the motion T_c.

By analyzing the response databank, the effect of the characteristics of the frames and the ground motions on the proposed relationship was identified. To this end, the expression

$$D = b_1 \cdot (n_s \cdot \lambda \cdot \alpha)^{b_2} \cdot \left(\frac{S_a}{g} \cdot \frac{T}{T_c} \right)^{b3} \tag{25}$$

with b_1, b_2, and b_3 constants to be determined, was selected as a good candidate for approximating the response databank. The aforementioned relation is relatively simple and satisfies the physical constraint $D=0$ for $S_a=0$. Use of the Levenberg–Marquardt algorithm [31] for nonlinear regression

analysis of the results of parametric studies, led to the following expressions for each one of the five damage indices:

$$D_{PA} = 0.42 \cdot (n_s \cdot \lambda \cdot \alpha)^{0.046} \cdot \left(\frac{S_a}{g} \cdot \frac{T}{T_c} \right)^{0.043} \quad (26)$$

$$D_{BRM} = 0.77 \cdot (n_s \cdot \lambda \cdot \alpha)^{0.051} \cdot \left(\frac{S_a}{g} \cdot \frac{T}{T_c} \right)^{0.083} \quad (27)$$

$$D_{RM} = 0.55 \cdot (n_s \cdot \lambda \cdot \alpha)^{0.020} \cdot \left(\frac{S_a}{g} \cdot \frac{T}{T_c} \right)^{0.043} \quad (28)$$

$$D_{CMR} = 0.43 \cdot (n_s \cdot \lambda \cdot \alpha)^{0.047} \cdot \left(\frac{S_a}{g} \cdot \frac{T}{T_c} \right)^{0.041} \quad (29)$$

$$D_{BV} = 0.42 \cdot (n_s \cdot \lambda \cdot \alpha)^{0.047} \cdot \left(\frac{S_a}{g} \cdot \frac{T}{T_c} \right)^{0.041} \quad (30)$$

With D being any damage index of interest, the mean, median and standard deviation of the ratio of the exact "value" of D obtained from inelastic dynamic analyses over the approximate one calculated from Eqs (26) to (30), respectively., i.e., D_{exact}/D_{app}, are used in order to express the central tendency and the dispersion of the error introduced by the proposed relations. Thus, for the Park and Ang damage index [13] the ratio $D_{PA.exact}/D_{PA,app}$ corresponds to a mean value equal to 1.00, a central value equal to 0.90 and a standard deviation equal to 0.32. Furthermore, this ratio corresponds to a mean value equal to 1.00, 1.00, 0.99 and 0.99, a central value equal to 0.99, 0.90, 0.89 and 0.90 and a standard deviation equal to 0.14, 0.36, 0.33 and 0.32 for the Bracci et al. [9], Roufaiel and Meyer [5], Cosenza et al. [6] and Banon and Veneziano [4] damage indices, respectively. Those values show that the proposed formulae are very accurate.

8. Examples of application

In this section, two numerical examples are presented in order to illustrate the use of the proposed expressions and demonstrate their advantages and precision by comparing the results derived by them with the "exact" values of damage obtained by nonlinear dynamic analysis.

8.1 Six storey moment resisting frame

A six storey-three bay MRF is examined, with a geometrical configuration similar to the one shown in Fig. 1. Gravity load on the beams is assumed equal to 27.5 kN/m (dead and live loads of floors), while the yield stress of the material is set equal to 235MPa. The frame has been designed in accordance with the provisions of structural Eurocodes EC3 [21] and EC8 [1]. The expected design ground motion was defined by the acceleration response spectrum of EC8 [1] with a PGA equal to 0.35 g, a soil of class B and a q factor equal to 4.0. The design yielded HEB280 and IPE360 sections for the columns and beams of the first four stories and HEB260 and IPE330 sections for the columns and beams of the next two higher stories, respectively.

The characteristic values ρ and α of the frame were computed on the basis of Equations (10) and (11) and found to be equal to 0.38 and 1.6, respectively. The fundamental period of vibration, T, of the frame is equal to 1.22 s, while its spectral acceleration S_a corresponding to this period, derived in the basis of EC8 [1] spectrum, equals 0.43 g.

Eight semi-artificial accelerograms compatible with the EC8 [1] spectrum were generated via a deterministic approach [32] on the basis of eight real seismic records of Table 3. The response spectra of these motions, in comparison with the EC8 [1] spectrum, are depicted in Fig. 4. Nonlinear time history analyses of the designed frame under these motions were performed. The five damage indices used here and observed in column bases and beams of the frame were computed with the aid of the program Ruaumoko 2D [18]. Then, the mean value of the maximum damage values for the eight semi-artificial accelerograms was evaluated for each damage index. Moreover, the approximate values of the damage indices were computed with the aid of Eqs (15)-(24) and recorded together with the exact ones in Tables 4 and 5 for column bases and beams, respectively. The proposed relations predict very well the damage of the beams (error = 3.3-6.4%) for all kinds of indices. A similar trend is observed for the columns (error = 0.7-6.5%) for all kinds of indices. Thus, the predictions of the proposed formulae are quite close to the "exact" ones and they are, in all cases, in the safe (conservative) side as being always larger than the "exact" ones.

8.2 Five storey x-braced frame

A five storey-three bay XBF frame is examined, with a geometrical configuration similar to the one shown in Fig. 2. Gravity load on the beams is assumed equal to 27.5 kN/m (dead and live loads of floors), while the yield stress of the material is set equal to 235MPa. The frame has been designed in accordance with the provisions of structural Eurocodes EC3 [21] and EC8 [1]. The expected design ground motion was defined by the acceleration response spectrum of EC8 [1] with a PGA equal to 0.24 g and a soil class B. A q factor equal to 4.0 was selected and the design procedure yielded HEB300 cross-sections for the columns, IPE330 cross-sections for the beams, TUBO-D193.7×4.5 cross-sections for the diagonals of the first two stories, TUBO-D168.3×4 cross-sections for the diagonals of the third storey, TUBO-D159×4 cross-sections for the diagonals of the fourth storey and TUBO-D133×4 for the diagonals of the fifth storey.

The characteristic values λ and α of the frame were computed on the basis of Equations (10) and (11) and found to be equal to 1.23 and 0.075, respectively. The fundamental period of vibration, T, of the frame and its spectral acceleration S_a corresponding to this period derived from EC8 [1] spectrum were equal to 0.55 s and 0.654 g, respectively, while the characteristic period, T_c equals 0.5 s. Eight semi-artificial accelerograms compatible with the EC8 spectrum were generated via a deterministic approach [32] on the basis of eight real seismic records of Table 3. The response spectra of these motions, in comparison with the EC8 [1] spectrum, are depicted in Fig. 5. Nonlinear time history analyses of the designed frame under these motions were performed. The five damage indices used here and are observed at the braces of the frame were computed with the aid of the program Ruaumoko 2D [18]. Then, the mean value of the maximum damage values the eight semi-artificial accelerograms was evaluated for each damage index. Moreover, the approximate values of the damage indices were computed with the aid of Eqs (26)-(30) and are recorded together with the "exact" ones in Table 6. It is observed that the approximate values of all the damage indices predicted by the proposed relationships are very close to the "exact" ones (error = 1.7-7.2%).

9. Conclusions

A procedure in terms of simple formulae for estimating the maximum damage in regular multi-storey moment resisting and x-braced steel frames subjected to ordinary (i.e. without near-fault effects) ground motions has been presented. Particularly, simple and easy to use relationships were derived for the computation of five damage indices of the literature, which take into account the influence of basic characteristics of moment resisting or x-braced steel frames and ground motions,

such as the number of stories, the period of vibration, stiffness ratio and capacity factor (for moment resisting frames), brace slenderness ratio and column stiffness (for x-braced frames), the spectral acceleration and the characteristic period. It should be noticed herein that the proposed relations are valid for frames with characteristics similar to those of the frames used in the parametric studies and for seismic sites where ordinary ground motions are expected. These expressions give a good approximation of damage and provide a rapid damage assessment of existing structures without the use of the more sophisticated and time consuming non-linear dynamic analysis. They can also be utilized in the preliminary design of structures in conjunction with elastic analysis in order to decrease the need for iterations of analysis/design. Finally, they can be useful when pushover analysis is performed, since cyclic accumulated damage can be predicted.

References

[1] EC8. Design of structures for earthquake resistance, Part 1: General rules, seismic actions and rules for buildings, European Standard EN 1998-1, European Committee for Standardization (CEN), Brussels, 1998.

[2] Fajfar P and Krawinkler H. Seismic Design Methodologies for the Next Generation of Codes. Bled, 24-27 June 1997, Balkema, Rotterdam.

[3] FEMA. FEMA-273 Building Seismic Safety Council, NEHRP guidelines for the seismic rehabilitation of buildings. Federal Emergency Management Agency, Washington (DC), 1997.

[4] Banon H, Veneziano D. Seismic safety of reinforced concrete members and structures. Earthquake Engineering and Structural Dynamics 1982; 10:179-173.

[5] Roufaiel MS Meyer C. Analytical modeling of hysteretic behavior of R/C frames. Journal of Structural Engineering, ASCE 1987; 113:429-444.

[6] Cosenza E, Manfredi G, Ramasco R. The use of damage functionals in earthquake engineering: A comparison between different methods. Earthquake Engineering and Structural Dynamics 1993; 22(10):855-868.

[7] Stephens JE, Yao JTP. Damage assessment using response measurements. Journal of Structural Engineering, ASCE 1987; 113:787-801.

[8] McCabe SL, Hall WJ. Assessment of seismic structural damage. Journal of Structural Engineering, ASCE 1989; 115: 2166-2183.

[9] Bracci JM, Reinhorn, AM, Mander JB. Deterministic model for seismic damage evaluation of reinforced concrete structures, Technical Report NCEER 89-0033, State University of New York at Buffalo, 1989.

[10] Krawinkler H, Zohrei M. Cumulative damage in steel structures subjected to earthquake ground motions. Computers and Structures 1983; 16:531-541.

[11] Sucuoğlu H, Erberik A. Energy-based hysteresis and damage models for deteriorating systems. Earthquake Engineering and Structural Dynamics 2004; 33: 69-88.

[12] Kamaris GS, Hatzigeorgiou GD, Beskos DE. A new damage index for plane steel frames exhibiting strength and stiffness degradation under seismic motion. Engineering Structures 2011; submitted.

[13] Park Y-J, Ang AH-S. Mechanistic seismic damage model for reinforced concrete. Journal of Structural Engineering, ASCE 1985; 111:722-739.

[14] Powell GH, Allahabadi R. Seismic damage prediction by deterministic methods: concepts and procedures. Earthquake Engineering and Structural Dynamics 1988; 16: 719-734.

[15] Lemaitre J. A Course on Damage Mechanics. Springer-Verlag, Berlin, 1992.

[16] Hatzigeorgiou GD, Beskos DE. Direct damage controlled design of concrete structures. Journal of Structural Engineering, ASCE 2007; 133:205-215.

[17] Kamaris GS, Hatzigeorgiou GD, Beskos DE. Direct damage controlled design of plane steel-moment resisting frames using static inelastic analysis. Journal of Mechanics of Materials and Structures 2009; 4:1375-1393.

[18] Carr AJ. RUAUMOKO-2D. Inelastic Time-History Analysis of Two-Dimensional Framed Structures, Department of Civil Engineering. University of Canterbury, New Zealand, 2006.

[19] Castiglioni CA, Pucinotti R. Failure criteria and cumulative damage models for steel components under cyclic loading. Journal of Constructional Steel Research 2009; 65:751-765.

[20] Akkar, S., Yazgan, U., and Gülkan, P., 2005. Drift estimates in frame buildings subjected to near-fault ground motions, J. Struct. Eng. 131, 1014–1024.

[21] EC3. Design of Steel Structures – Part 1-1: General Rules for Buildings, ENV1993-1-1, European Standard EN 1998-1, European Committee for Standardization (CEN), Brussels, 1992.

[22] Karavasilis TL, Bazeos N, Beskos DE (2008). Drift and Ductility Estimates in Regular Steel MRF Subjected to Ordinary Ground Motions: A Design-Oriented Approach. Earthquake Spectra 24(2):431-451.

[23] Androic B, Dzeba I, Dujmovic D. International Structural Steel Sections: Design Tables According to Eurocode 3. Ernst & Sohn: Berlin, 2000.

[24] MacRae GA, Kimura Y, Roeder C. Effect of column stiffness on braced frame seismic behavior. Journal of Structural Engineering (ASCE) 2004; 130(3):381–391.

[25] Kimura Y, MacRae GA. Effect of column flexural characteristic on seismic behavior of braced frame with fixed column base. Behavior of Steel Structures in Seismic Area, Proceedings of the STESSA 2006 Conference, Mazzolani F, Wada A (eds). Taylor & Francis: Yokohama, Japan, August 2006; 437–443.

[26] Karavasilis TL, Bazeos N, Beskos DE. Estimation of seismic drift and ductility demands in planar regular x-braced steel frames. Earthquake Engineering and Structural Dynamics 2007; 36:2273–2289.

[27] Vallianatou YM, M.S. Thesis, Department of Civil Engineering, University of Patras, Patras, Greece, 2011 (in Greek).

[28] PEER Pacific earthquake engineering research centre. Strong ground motion database: http://peer.berkeley.edu/, 2006.

[29] Riddell R, Newmark NM. Statistical analysis of the response of nonlinear systems subjected to earthquakes. Structural Research Series No. 468, Department of Civil Engineering, University of Illinois, Urbana, 1979.

[30] Remennikov A.M. and Walpole W.R. Analytical Prediction of seismic behavior for concentrically-braced steel systems. Earthquake Engineering and Structural Dynamics 1997; 26:859-874.

[31] MATLAB. The language of technical computing, Version 5.0. The Mathworks Inc., Natick, Mass, 1997.

[32] Karabalis DL, Cokkinides GJ, Rizos DC. Seismic Record Processing Program-Ver.1.03,

Report of the College of Engineering, University of South Carolina, Columbia, 1992.

Table 1. Steel moment resisting frames considered in parametric studies.

General data				Sections	Periods	
n_s	n_b	ρ	a	Columns: (HEB) & Beams: (IPE)	T_1(sec)	T_2(sec)
3	3	0.47	1.30	240-330(1-3)	0.73	0.26
3	3	0.36	1.60	260-330(1-3)	0.69	0.21
3	3	0.28	1.90	280-330(1-3)	0.65	0.19
3	3	0.21	2.30	300-330(1-3)	0.62	0.18
3	3	0.29	1.80	300-360(1-3)	0.57	0.16
3	6	0.54	1.30	240-330(1-3)	0.75	0.23
3	6	0.41	1.60	260-330(1-3)	0.70	0.21
3	6	0.31	1.90	280-330(1-3)	0.66	0.20
3	6	0.24	2.30	300-330(1-3)	0.63	0.19
6	3	0.38	1. 60	280-360(1-4)+260-330(5-6)	1.22	0.41
6	3	0.29	1.97	300-360(1-4)+280-330(5-6)	1.17	0.38
6	3	0.24	2.27	320-360(1-4)+300-330(5-6)	1.13	0.37
6	3	0.20	2.54	340-360(1-4)+300-330(5-6)	1.11	0.36
6	3	0.20	2.54	340-360(1-4)+320-330(5-6)	1.10	0.35
6	6	0.43	1.60	280-360(1-4)+260-330(5-6)	1.25	0.42
6	6	0.33	1.97	300-360(1-4)+280-330(5-6)	1.19	0.40
6	6	0.27	2.27	320-360(1-4)+300-330(5-6)	1.15	0.38
6	6	0.23	2.54	340-360(1-4)+300-330(5-6)	1.12	0.37
9	3	0.28	2.19	340-360(1)+340-400(2-5)+320-360(6-7)+300-330(8-9)	1.55	0.54
9	3	0.24	2.43	360-360(1)+360-400(2-5)+340-360(6-7)+320-330(8-9)	1.52	0.53
9	3	0.18	2.93	400-360(1)+400-400(2-5)+360-360(6-7)+340-330(8-9)	1.46	0.51
9	3	0.18	3.62	450-360(1)+400-400(2-5)+360-360(6-7)+340-330(8-9)	1.45	0.50
9	3	0.18	1.83	450-360(1)+450-450(2-5)+360-360(6-7)+340-330(8-9)	1.28	1.28
9	6	0.32	2.19	340-360(1)+340-400(2-5)+320-360(6-7)+300-330(8-9)	1.57	0.55
9	6	0.28	2.43	360-360(1)+360-400(2-5)+340-360(6-7)+320-330(8-9)	1.53	0.53
9	6	0.21	2.93	400-360(1)+400-400(2-5)+360-360(6-7)+340-330(8-9)	1.47	0.51
9	6	0.21	3.62	450-360(1)+400-400(2-5)+360-360(6-7)+340-330(8-9)	1.45	0.50
12	3	0.24	2.60	400-360(1)+400-400(2-3)+400-450(4-5)+ 360-400(6-7)+340-400(8-9)+340- 360(10)+340-330(11-12)	1.90	0.66
12	3	0.26	3.00	450-360(1)+450-400(2-3)+450-450(4-5) +400-450(6-7)+360-400(8-9) +360-360(10)+360-330(11-12)	1.78	0.62
12	3	0.19	3.63	500-360(1)+500-400(2-3)+500-450(4-5) +450-450(6-7)+400-400(8-9)+ 400-360(10-11)+400-330(12)	1.72	0.60
12	3	0.14	4.22	550-360(1)+550-400(2-3)+550-450(4-5) +500-450(6-7)+400-400(8-9)+ 400-360(10-11)+400-330(12)	1.67	0.59
12	3	0.20	3.54	550-400(1)+550-450(2-3)+550-500(4-5) +500-500(6-7)+400-400(8-9)+ 400-360(10-11)+400-330(12)	1.51	0.56
12	6	0.28	2.60	400-360(1)+400-400(2-3)+400-450(4-5) +360-400(6-7)+340-400(8-9) +340-360(10)+340-330(11-12)	1.90	0.67

Table 1. (Continued).

General data				Sections	Periods	
n_s	n_b	ρ	a	Columns: (HEB) & Beams: (IPE)	T_1(sec)	T_2(sec)
12	6	0.30	3.00	450-360(1)+450-400(2-3)+450-450(4-5) +400-450(6-7)+360-400(8-9) +360-360(10)+360-330(11-12)	1.78	0.63
12	6	0.22	3.63	500-360(1)+500-400(2-3)+500-450(4-5) +450-450(6-7)+400-400(8-9) +400-360(10-11)+400-330(12)	1.72	0.61
12	6	0.16	4.22	550-360(1)+550-400(2-3)+550-450(4-5) +500-450(6-7)+400-400(8-9)+ 400-360(10-11)+400-330(12)	1.56	0.59
15	3	0.13	3.87	500-300(1)+500-400(2-3)+500-450(4-5) +450-400(6-7)+400-400(8-12) +400-360(13-14)+400-330(15)	2.29	0.78
15	3	0.10	4.49	550-300(1)+550-400(2-3)+550-450(4-5) +500-400(6-7)+450-400(8-12) +450-360(13-14)+450-330(15)	2.22	0.75
15	3	0.11	4.76	600-300(1)+600-400(2-3)+600-450(4-5) +550-450(6-7)+500-450(8-9)+500-400(10-12) +500-360(13-14)+500-330(15)	2.10	0.72
15	3	0.09	5.43	650-300(1)+600-400(2-3)+600-450(4-5) +600-450(6-7)+500-450(8-9)+500-400(10-12) +500-360(13-14)+500-330(15)	2.03	0.70
15	3	0.07	5.23	650-300(1)+650-450(2-3)+650-450(4-5) +650-450(6-7)+500-450(8-9)+500-400(10-12) +500-360(13-14)+500-330(15)	1.96	0.68
15	6	0.15	3.87	500-300(1)+500-400(2-3)+500-450(4-5) +450-400(6-7)+400-400(8-12) +400-360(13-14)+400-330(15)	2.30	0.78
15	6	0.11	4.49	550-300(1)+550-400(2-3)+550-450(4-5) +500-400(6-7)+450-400(8-12) +450-360(13-14)+450-330(15)	2.21	0.75
15	6	0.13	4.76	600-300(1)+600-400(2-3)+600-450(4-5) +550-450(6-7)+500-450(8-9)+500-400(10-12) +500-360(13-14)+500-330(15)	2.10	0.72
15	6	0.10	5.43	650-300(1)+600-400(2-3)+600-450(4-5) +600-450(6-7)+500-450(8-9)+500-400(10-12) +500-360(13-14)+500-330(15)	1.88	0.68
20	3	0.11	4.54	600-300(1)+600-400(2-3)+600-450(4-5) +550-450(6-10)+500-450(11-13)+500-400(14-16) +450-400(17)+450-360(18-19)+450-330(20)	2.82	0.97
20	3	0.09	5.16	650-300(1)+650-400(2-3)+650-450(4-5) +600-450(6-10)+550-450(11-13)+550-400(14-16) +500-400(17)+500-360(18-19)+500-330(20)	2.76	0.94
20	3	0.07	5.90	700-300(1)+700-360(2)+700-400(3)+700-450(4-5) +650-450(6-10)+600-450(11-13)+600-400(14-16) +550-400(17)+550-360(18-19)+550-330(20)	2.73	0.93
20	3	0.06	7.27	800-300(1)+800-360(2)+800-400(3)+800-450(4-5) +700-450(6-10)+600-450(11-13)+600-400(14-16) +550-400(17)+550-360(18-19)+550-330(20)	2.62	0.90
20	3	0.04	7.17	800-360(1)+800-360(2)+800-400(3)+800-450(4-5) +800-450(6-10)+600-450(11-13)+600-400(14-16) +550-400(17)+550-360(18-19)+550-330(20)	2.60	0.89
20	6	0.13	4.54	600-300(1)+600-400(2-3)+600-450(4-5) +550-450(6-10)+500-450(11-13)+500-400(14-16) +450-400(17)+450-360(18-19)+450-330(20)	2.75	0.96
20	6	0.10	5.16	650-300(1)+650-400(2-3)+650-450(4-5) +600-450(6-10)+550-450(11-13)+550-400(14-16) +500-400(17)+500-360(18-19)+500-330(20)	2.70	0.93
20	6	0.08	5.90	700-300(1)+700-360(2)+700-400(3)+700-450(4-5) +650-450(6-10)+600-450(11-13)+600-400(14-16) +550-400(17)+550-360(18-19)+550-330(20)	2.67	0.92
20	6	0.07	7.27	800-300(1)+800-360(2)+800-400(3)+800-450(4-5) +700-450(6-10)+600-450(11-13)+600-400(14-16) +550-400(17)+550-360(18-19)+550-330(20)	2.57	0.89

Table 2. Structural data of the x-braced steel frames considered in parametric studies.

General data			Periods	Sections	
n_s	λ	α	T	Columns (HEB)	Braces (TUBO)
3	1.93	0.04	0.41	220+220+220	(127x4)+(108x3.6)+(101.6x3.6)
3	1.93	0.10	0.40	280+280+280	(127x4)+(108x3.6)+(101.6x3.6)
3	1.93	0.19	0.40	340+340+340	(127x4)+(108x3.6)+(101.6x3.6)
3	1.56	0.04	0.36	240+240+240	(152.4x4)+(133x4)+(127x4)
3	1.56	0.10	0.36	300+300+300	(152.4x4)+(133x4)+(127x4)
3	1.56	0.17	0.35	360+360+360	(152.4x4)+(133x4)+(127x4)
3	1.30	0.05	0.32	260+260+260	(193.7x4.5)+(159x4)+(139.7x4)
3	1.30	0.10	0.32	320+320+320	(193.7x4.5)+(159x4)+(139.7x4)
3	1.30	0.18	0.31	400+400+400	(193.7x4.5)+(159x4)+(139.7x4)
6	1.93	0.04	0.83	240+240+220+220+200+200	(127x4)+(127x4)+(127x4)+(108x3.6)+(101.6x3.6)+(82.5x3.2)
6	1.93	0.10	0.79	300+300+280+280+260+260	(127x4)+(127x4)+(127x4)+(108x3.6)+(101.6x3.6)+(82.5x3.2)
6	1.93	0.19	0.77	360+360+340+340+320+320	(127x4)+(127x4)+(127x4)+(108x3.6)+(101.6x3.6)+(82.5x3.2)
6	1.56	0.04	0.75	260+260+240+240+220+220	(152.4x4)+(152.4x4)+(139.7x4)+(133x4)+(127x4)+(101.6x3.6)
6	1.56	0.10	0.72	320+320+300+300+280+280	(152.4x4)+(152.4x4)+(139.7x4)+(133x4)+(127x4)+(101.6x3.6)
6	1.56	0.17	0.70	400+400+360+360+340+340	(152.4x4)+(152.4x4)+(139.7x4)+(133x4)+(127x4)+(101.6x3.6)
6	1.30	0.05	0.68	280+280+260+260+240+240	(193.7x4.5)+(193.7x4.5)+(168.3x4)+(159.4)+(139.7x4)+(127x4)
6	1.30	0.10	0.65	340+340+320+320+300+300	(193.7x4.5)+(193.7x4.5)+(168.3x4)+(159.4)+(139.7x4)+(127x4)
6	1.30	0.18	0.63	450+450+400+400+360+360	(193.7x4.5)+(193.7x4.5)+(168.3x4)+(159.4)+(139.7x4)+(127x4)
9	1.93	0.06	1.37	260+260+260+240+240+240+220+220+220	(127x4)+(127x4)+(127x4)+(127x4)+(108x3.6)+(108x3.6)+(101.6x3.6)+(88.9x3.2)+(76.1x3.2)
9	1.93	0.10	1.31	300+300+300+280+280+280+260+260+260	(127x4)+(127x4)+(127x4)+(127x4)+(108x3.6)+(108x3.6)+(101.6x3.6)+(88.9x3.2)+(76.1x3.2)
9	1.93	0.19	1.26	360+360+360+340+340+340+320+320+320	(127x4)+(127x4)+(127x4)+(127x4)+(108x3.6)+(108x3.6)+(101.6x3.6)+(88.9x3.2)+(76.1x3.2)
9	1.56	0.06	1.24	280+280+280+260+260+260+240+240+240	(152.4x4)+(152.4x4)+(152.4x4)+(139.7x4)+(133x4)+(127x4)+(127x4)+(108x3.6)+(88.9x3.2)
9	1.56	0.10	1.19	320+320+320+300+300+300+280+280+280	(152.4x4)+(152.4x4)+(152.4x4)+(139.7x4)+(133x4)+(127x4)+(127x4)+(108x3.6)+(88.9x3.2)
9	1.56	0.17	1.14	400+400+400+360+360+360+340+340+340	(152.4x4)+(152.4x4)+(152.4x4)+(139.7x4)+(133x4)+(127x4)+(127x4)+(108x3.6)+(88.9x3.2)
9	1.30	0.08	1.10	320+320+320+300+300+300+280+280+280	(193.7x4.5)+(193.7x4.5)+(193.7x4.5)+(193.7x4.5)+(159x4)+(152.4x4)+(139.7x4)+(127x4)+(108x3.6)
9	1.30	0.14	1.04	400+400+400+360+360+360+340+340+340	(193.7x4.5)+(193.7x4.5)+(193.7x4.5)+(193.7x4.5)+(159x4)+(152.4x4)+(139.7x4)+(127x4)+(108x3.6)
9	1.30	0.18	1.02	450+450+450+400+400+400+360+360+360	(193.7x4.5)+(193.7x4.5)+(193.7x4.5)+(193.7x4.5)+(159x4)+(152.4x4)+(139.7x4)+(127x4)+(108x3.6)
12	1.93	0.10	1.92	320+320+320+300+300+300+280+280+280+260+260+260	(127x4)+(127x4)+(127x4)+(127x4)+(127x4)+(108x3.6)+(108x3.6)+(101.6x3.6)+(101.6x3.6)+(101.6x3.6)+(82.5x3.2)+(76.1x3.2)
12	1.93	0.19	1.83	400+400+400+360+360+360+340+340+340+320+320+320	(127x4)+(127x4)+(127x4)+(127x4)+(127x4)+(108x3.6)+(108x3.6)+(101.6x3.6)+(101.6x3.6)+(101.6x3.6)+(82.5x3.2)+(76.1x3.2)
12	1.93	0.23	1.79	450+450+450+400+400+400+360+360+360+340+340+340	(127x4)+(127x4)+(127x4)+(127x4)+(127x4)+(108x3.6)+(108x3.6)+(101.6x3.6)+(101.6x3.6)+(101.6x3.6)+(82.5x3.2)+(76.1x3.2)
12	1.56	0.12	1.74	360+360+360+340+340+340+320+320+320+300+300+300	(152.4x4)+(152.4x4)+(152.4x4)+(152.4x4)+(139.7x4)+(133x4)+(133x4)+(127x4)+(127x4)+(108x3.6)+(101.6x3.6)+(82.5x3.2)
12	1.56	0.17	1.66	450+450+450+400+400+400+360+360+360+340+340+340	(152.4x4)+(152.4x4)+(152.4x4)+(152.4x4)+(139.7x4)+(133x4)+(133x4)+(127x4)+(127x4)+(108x3.6)+(101.6x3.6)+(82.5x3.2)
12	1.56	0.22	1.63	500+500+500+450+450+450+400+400+400+360+360+360	(152.4x4)+(152.4x4)+(152.4x4)+(152.4x4)+(139.7x4)+(133x4)+(133x4)+(127x4)+(127x4)+(108x3.6)+(101.6x3.6)+(82.5x3.2)
12	1.30	0.12	1.60	400+400+400+360+360+360+340+340+340+320+320+320	(193.7x4.5)+(193.7x4.5)+(193.7x4.5)+(193.7x4.5)+(193.7x4.5)+(168.3x4)+(159x4)+(152.4x4)+(139.7x4)+(133x4)+(127x4)+(101.6x3.6)
12	1.30	0.18	1.52	500+500+500+450+450+450+400+400+400+360+360+360	(193.7x4.5)+(193.7x4.5)+(193.7x4.5)+(193.7x4.5)+(193.7x4.5)+(168.3x4)+(159x4)+(152.4x4)+(139.7x4)+(133x4)+(127x4)+(101.6x3.6)
12	1.30	0.25	1.49	550+550+550+500+500+500+450+450+450+400+400+400	(193.7x4.5)+(193.7x4.5)+(193.7x4.5)+(193.7x4.5)+(193.7x4.5)+(168.3x4)+(159x4)+(152.4x4)+(139.7x4)+(133x4)+(127x4)+(101.6x3.6)

Table 2. (Continued).

General data			Periods	Sections	
n_s	λ	α	T	Columns (HEB)	Braces (TUBO)
15	1.93	0.19	2.62	400+400+400+360+360+360+340+340 +340+320+320+320+300+300+300	(127x4)+(127x4)+(114.3x3.6)+(114.3x3.6)+(114.3x3.6)+(114.3x3.6)+(10 8x3.6)+(108x3.6)+(101.6x3.6)+(101.6x3.6)+(101.6x3.6)+(88.9x3.2)+(82. 5x3.2)+(76.1x3.2)+(76.1x3.2)
15	1.93	0.23	2.55	450+450+450+400+400+400+360+360 +360+340+340+340+320+320+320	(127x4)+(127x4)+(114.3x3.6)+(114.3x3.6)+(114.3x3.6)+(114.3x3.6)+(10 8x3.6)+(108x3.6)+(101.6x3.6)+(101.6x3.6)+(101.6x3.6)+(88.9x3.2)+(82. 5x3.2)+(76.1x3.2)+(76.1x3.2)
15	1.93	0.30	2.49	500+500+500+450+450+450+400+400 +400+360+360+360+340+340+340	(127x4)+(127x4)+(114.3x3.6)+(114.3x3.6)+(114.3x3.6)+(114.3x3.6)+(10 8x3.6)+(108x3.6)+(101.6x3.6)+(101.6x3.6)+(101.6x3.6)+(88.9x3.2)+(82. 5x3.2)+(76.1x3.2)+(76.1x3.2)
15	1.56	0.17	2.39	450+450+450+400+400+400+360+360 +360+340+340+340+320+320+320	(152.4x4)+(152.4x4)+(152.4x4)+(152.4x4)+(139.7x4)+(139.7x4)+(133x4)+(133x4)+(127x4)+(127x4)+(127x4)+(108x3.6)+(101.6x3.6)+(88.9x3.2) +(76.1x3.2)
15	1.56	0.22	2.32	500+500+500+450+450+450+400+400 +400+360+360+360+340+340+340	(152.4x4)+(152.4x4)+(152.4x4)+(152.4x4)+(139.7x4)+(139.7x4)+(133x4)+(133x4)+(127x4)+(127x4)+(127x4)+(108x3.6)+(101.6x3.6)+(88.9x3.2) +(76.1x3.2)
15	1.56	0.30	2.27	550+550+550+500+500+500+450+450 +450+400+400+400+360+360+360	(152.4x4)+(152.4x4)+(152.4x4)+(152.4x4)+(139.7x4)+(139.7x4)+(133x4)+(133x4)+(127x4)+(127x4)+(127x4)+(108x3.6)+(101.6x3.6)+(88.9x3.2) +(76.1x3.2)
15	1.30	0.34	2.08	600+600+600+550+550+550+500+500 +500+450+450+450+400+400+400	(193.7x4.5)+(193.7x4.5)+(193.7x4.5)+(193.7x4.5)+(193.7x4.5)+(168.3x4)+(168.3x4)+(159x4)+(152.4x4)+(152.4x4)+(139.7x4)+(133x4)+(127x4) +(108x3.6)+(101.6x3.6
15	1.30	0.44	2.04	650+650+650+600+600+600+550+550 +550+500+500+500+450+450+450	(193.7x4.5)+(193.7x4.5)+(193.7x4.5)+(193.7x4.5)+(193.7x4.5)+(168.3x4)+(168.3x4)+(159x4)+(152.4x4)+(152.4x4)+(139.7x4)+(133x4)+(127x4) +(108x3.6)+(101.6x3.6
15	1.30	0.54	2.00	700+700+700+650+650+650+600+600 +600+550+550+550+500+500+500	(193.7x4.5)+(193.7x4.5)+(193.7x4.5)+(193.7x4.5)+(193.7x4.5)+(168.3x4)+(168.3x4)+(159x4)+(152.4x4)+(152.4x4)+(139.7x4)+(133x4)+(127x4) +(108x3.6)+(101.6x3.6)
20	1.93	0.72	3.65	650+650+650+650+600+600+600+600 +550+550+550+550+500+500+500+ 500+450+450+450+450	(127x4)+(127x4)+(127x4)+(127x4)+(114.3x3.6)+(114.3x3.6)+(114.3x3.6)+(114.3x3.6)+(108x3.6)+(108x3.6)+(108x3.6)+(101.6x3.6)+(101.6x3.6) +(101.6x3.6)+(101.6x3.6)+(88.9x3.2)+(82.5x3.2)+(76.1x3.2)+(76.1x3.2)+ (76.1x3.2)
20	1.93	0.9	3.58	700+700+700+700+650+650+650+650 +600+600+600+600+550+550+550+ 550+500+500+500+500	(127x4)+(127x4)+(127x4)+(127x4)+(114.3x3.6)+(114.3x3.6)+(114.3x3.6)+(114.3x3.6)+(108x3.6)+(108x3.6)+(108x3.6)+(101.6x3.6)+(101.6x3.6) +(101.6x3.6)+(101.6x3.6)+(88.9x3.2)+(82.5x3.2)+(76.1x3.2)+(76.1x3.2)+ (76.1x3.2)
20	1.93	1.1	3.49	800+800+800+800+700+700+700+700 +650+650+650+650+600+600+600+ 600+550+550+550+550	(127x4)+(127x4)+(127x4)+(127x4)+(114.3x3.6)+(114.3x3.6)+(114.3x3.6)+(114.3x3.6)+(108x3.6)+(108x3.6)+(108x3.6)+(101.6x3.6)+(101.6x3.6) +(101.6x3.6)+(101.6x3.6)+(88.9x3.2)+(82.5x3.2)+(76.1x3.2)+(76.1x3.2)+ (76.1x3.2)
20	1.56	0.65	3.36	700+700+700+700+650+650+650+650 +600+600+600+600+550+550+550+ 550+500+500+500+500	(159x4)+(152.4x4)+(152.4x4)+(152.4x4)+(152.4x4)+(152.4x4)+(152.4x4)+(139.7x4)+(139.7x4)+(139.7x4)+(133x4)+(127x4)+(127x4)+(127x4)+(114.3x3.6)+(114.3x3.6)+(108x3.6)+(101.6x3.6)+(88.9x3.2)+(76.1x3.2)
20	1.56	0.81	3.27	800+800+800+800+700+700+700+700 +650+650+650+650+600+600+600+ 600+550+550+550+550	(159x4)+(152.4x4)+(152.4x4)+(152.4x4)+(152.4x4)+(152.4x4)+(152.4x4)+(139.7x4)+(139.7x4)+(139.7x4)+(133x4)+(127x4)+(127x4)+(127x4)+(114.3x3.6)+(114.3x3.6)+(108x3.6)+(101.6x3.6)+(88.9x3.2)+(76.1x3.2
20	1.56	0.98	3.17	900+900+900+900+800+800+800+800 +700+700+700+700+650+650+650+ 650+600+600+600+600	(159x4)+(152.4x4)+(152.4x4)+(152.4x4)+(152.4x4)+(152.4x4)+(152.4x4)+(139.7x4)+(139.7x4)+(139.7x4)+(133x4)+(127x4)+(127x4)+(127x4)+(114.3x3.6)+(114.3x3.6)+(108x3.6)+(101.6x3.6)+(88.9x3.2)+(76.1x3.2)
20	1.30	0.67	3.11	800+800+800+800+700+700+700+700 +650+650+650+650+600+600+600+ 600+550+550+550+550	(193.7x4.5)+(193.7x4.5)+(193.7x4.5)+(193.7x4.5)+(193.7x4.5)+(193.7x4 .5)+(193.7x4.5)+(168.3x4)+(168.3x4)+(159x4)+(159x4)+(152.4x4)+(152. 4x4)+(152.4x4)+(133x4)+(127x4)+(127x4)+(127x4)+(101.6x3.6)+(101.6x3.6)
20	1.30	0.82	3.00	900+900+900+900+800+800+800+800 +700+700+700+700+650+650+650+ 650+600+600+600+600	(193.7x4.5)+(193.7x4.5)+(193.7x4.5)+(193.7x4.5)+(193.7x4.5)+(193.7x4 .5)+(193.7x4.5)+(168.3x4)+(168.3x4)+(159x4)+(159x4)+(152.4x4)+(152. 4x4)+(152.4x4)+(133x4)+(127x4)+(127x4)+(127x4)+(101.6x3.6)+(101.6 x3.6)
20	1.30	1.14	2.91	1000+1000+1000+1000+900+900+900+ 900+800+800+800+800+700+700+700 +700+650+650+650+650	(193.7x4.5)+(193.7x4.5)+(193.7x4.5)+(193.7x4.5)+(193.7x4.5)+(193.7x4 .5)+(193.7x4.5)+(168.3x4)+(168.3x4)+(159x4)+(159x4)+(152.4x4)+(152. 4x4)+(152.4x4)+(133x4)+(127x4)+(127x4)+(127x4)+(101.6x3.6)+(101.6 x3.6)

Table 3. Characteristics of ground motions used in parametric studies.

No	Date	Record Name	Comp.	Station Name	PGA (g)	Tc (s)
1.	1992/04/25	Cape Mendocino	NS	89509 Eureka	0.154	0.52
2.	1992/04/25	Cape Mendocino	EW	89509 Eureka	0.178	0.89
3.	1980/06/09	Victoria, Mexico	N045	6604 Cerro Prieto	0.621	0.56
4.	1980/06/09	Victoria, Mexico	N135	6604 Cerro Prieto	0.587	0.37
5.	1992/04/25	Cape Mendocino	EW	89324 Rio Dell Overpass	0.385	0.50
6.	1992/04/25	Cape Mendocino	NS	89324 Rio Dell Overpass	0.549	0.44
7.	1978/08/13	Santa Barbara	N048	283 Santa Barbara Courthouse	0.203	0.58
8.	1978/08/13	Santa Barbara	N138	283 Santa Barbara Courthouse	0.102	0.41
9.	1999/09/20	Chi-Chi, Taiwan	NS	TCU095	0.712	0.33
10.	1999/09/20	Chi-Chi, Taiwan	NS	TCU095	0.378	0.44
11.	1979/08/06	Coyote Lake	N213	1377 San Juan Bautista	0.108	0.41
12.	1979/08/06	Coyote Lake	N303	1377 San Juan Bautista	0.107	0.48
13.	1994/01/17	Northridge	NS	90021 LA - N Westmoreland	0.361	0.38
14.	1994/01/17	Northridge	EW	90021 LA - N Westmoreland	0.401	0.29
15.	1986/07/08	N.Palm Springs	NS	12204 San Jacinto - Soboba	0.239	0.20
16.	1986/07/08	N.Palm Springs	EW	12204 San Jacinto - Soboba	0.250	0.20
17.	1970/09/12	Lytle Creek	N115	290 Wrightwood	0.162	0.40
18.	1970/09/12	Lytle Creek	N205	290 Wrightwood	0.200	0.29
19.	1989/10/18	Loma Prieta	NS	58065 Saratoga - Aloha Ave	0.324	0.39
20.	1989/10/18	Loma Prieta	EW	58065 Saratoga - Aloha Ave	0.512	0.52
21.	1992/06/28	Landers	NS	22170 Joshua Tree	0.284	0.70
22.	1992/06/28	Landers	EW	22170 Joshua Tree	0.274	0.83
23.	1976/09/15	Friuli, Italy	NS	8014 Forgaria Cornino	0.212	0.26
24.	1976/09/15	Friuli, Italy	EW	8014 Forgaria Cornino	0.260	0.23
25.	1999/09/20	Chi-Chi, Taiwan	N045	TCU045	0.512	0.50
26.	1989/10/22	Loma Prieta	EW	1678 Golden Gate Bridge	0.233	1.00
27.	1994/01/17	Northridge	EW	24538 Santa Monica City Hall	0.883	0.23
28.	1994/01/17	Northridge	N279	90013 Beverly Hills- 14145 Mulhol	0.516	0.55
29.	1994/01/17	Northridge	NS	90047 Playa Del Rey - Saran	0.136	0.85
30.	1994/01/17	Northridge	EW	24401 San Marino, SW Academy	0.116	0.27
31.	1952/07/21	Kern country	N111	Taft	0.178	0.44
32.	1971/02/09	San Fernando	N291	Castaic	0.268	0.50
33.	1992/06/28	Landers	NS	Desert Hot Springs	0.171	0.46
34.	1994/01/17	Northridge	EW	Castaic-Old Ridge Route	0.568	0.44
35.	1994/01/17	Northridge	NS	Hollywood-Willoughby Ave	0.245	0.88
36.	1994/01/17	Northridge	N070	90015 LA - Chalon Rd	0.225	0.43
37.	1994/01/17	Northridge	EW	LA-Century City CC North	0.256	0.38
38.	1994/01/17	Northridge	EW	24400 LA - Obregon Park	0.355	0.24
39.	1994/01/17	Northridge	NS	24157 LA - Baldwin Hills	0.168	0.37
40.	1994/01/17	Northridge	N352	Big Tujunga, Angeles Nat F	0.245	0.21

Table 4. Comparison between "exact" and approximate values of damage indices for columns of the MRF.

Damage Index	"Exact" Value	Approximate Value	Error(%)
D_{PAM}	0.185	0.192	3.6
D_{BRM}	0.263	0.272	3.3
D_{RMO}	0.138	0.146	5.5
D_{CMR}	0.119	0.126	5.6
D_{BVM}	0.234	0.250	6.4

Table 5. Comparison between "exact" and approximate values of damage indices for beams of the MRF.

Damage Index	"Exact" Value	Approximate Value	Error(%)
D_{PAM}	0.322	0.344	6.4
D_{BRM}	0.238	0.242	1.7
D_{RMO}	0.286	0.288	0.7
D_{CMR}	0.215	0.230	6.5
D_{BVM}	0.395	0.402	1.7

Table 6. Comparison between "exact" and approximate values of damage indices of the XBF.

Damage Index	"Exact" Value	Approximate Value	Error(%)
D_{PAM}	0.416	0.430	4.1
D_{BRM}	0.776	0.720	7.2
D_{RMO}	0.525	0.534	1.7
D_{CMR}	0.395	0.409	3.4
D_{BVM}	0.407	0.399	2.0

Captions of figures

Figure 1. Geometrical configuration of the MRFs considered in this investigation.

Figure 2. Geometrical configuration of the XBFs considered in this investigation.

Figure 3. Response spectra of ground motions considered in parametric studies.

Figure 4. Response spectra of ground motions used in example of sec 8.1.

Figure 5. Response spectra of ground motions used in example of sec 8.2.

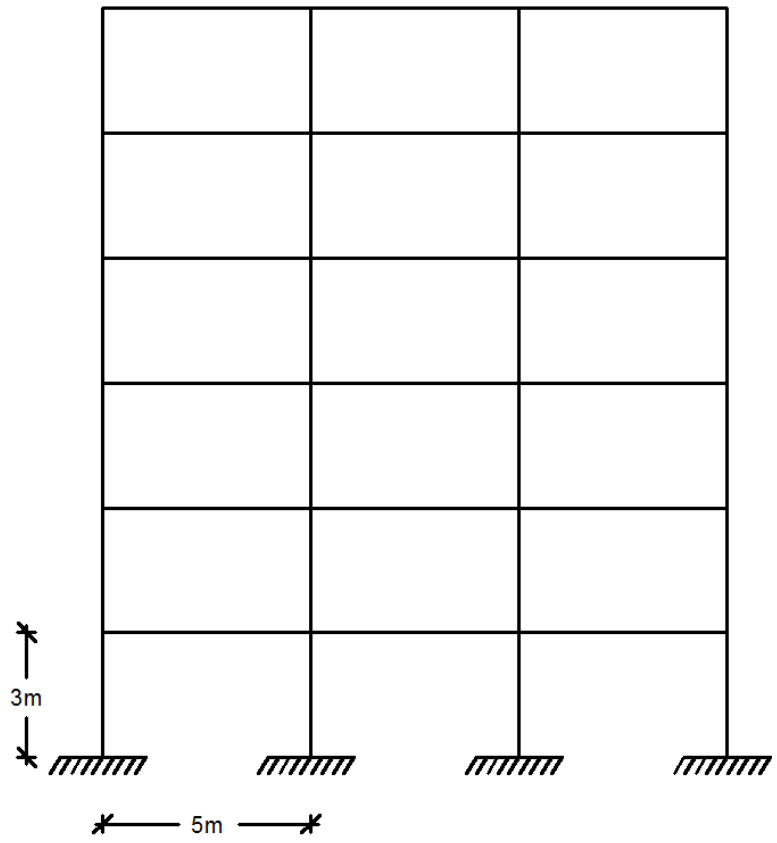

Figure 1

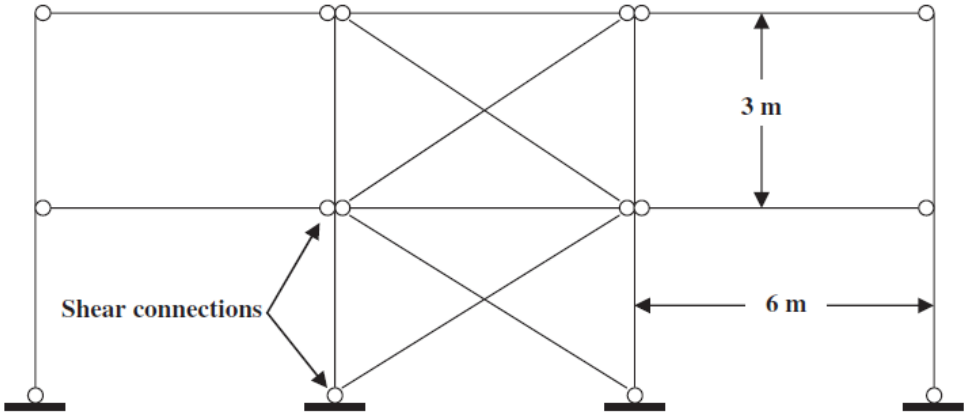

Figure 2

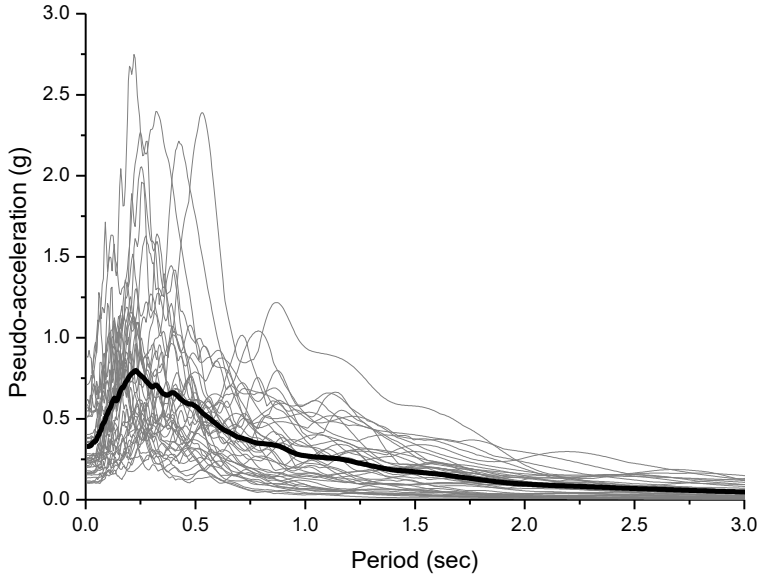

Figure 3

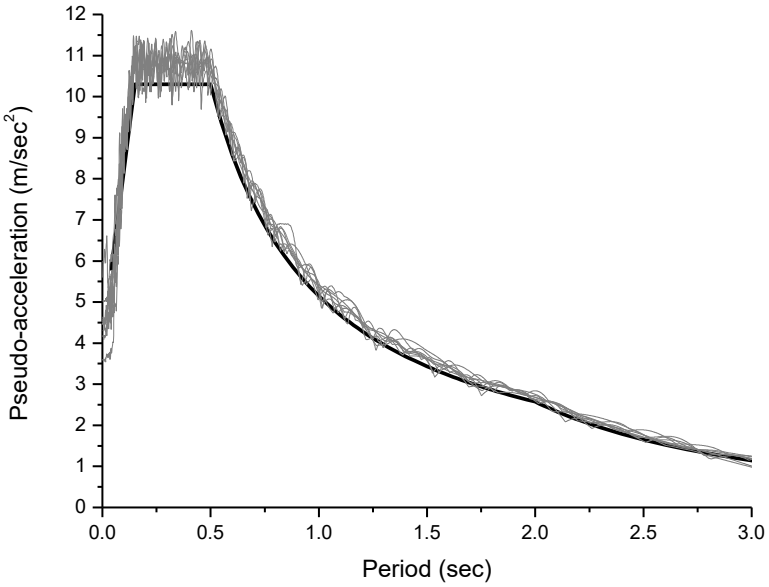
Pseudo-acceleration (m/sec^2)
Period (sec)
0
1
2
3
4
5
6
7
8
9
10
11
12
0.0
0.5
1.0
1.5
2.0
2.5
3.0

Figure 4

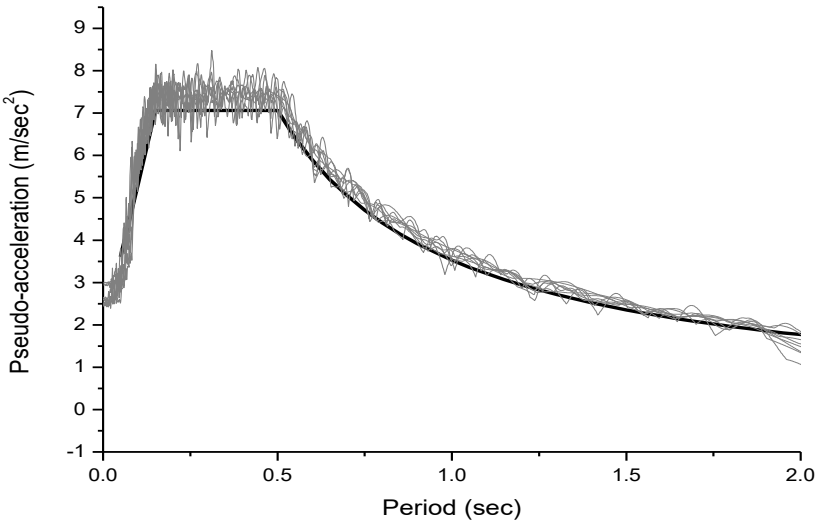
Pseudo-acceleration (m/sec^2)
9
8
7
6
5
4
3
2
1
0
-1
0.0
0.5
1.0
1.5
2.0
Period (sec)

Figure 5